

High-Frequency Sequence Stratigraphy and Fine-Scale Reservoir Characterization of the Devonian Sandstone, Donghe Formation, North Uplift of the Tarim Basin

WANG Ziyuan¹, LIU Li^{2,*}, PAN Mao¹, SHI Yongmin¹ and XIONG Fengyang³

¹ School of Earth and Space Sciences, Peking University, Beijing 100871, China

² Bureau of Economic Geology, Jackson School of Geosciences, The University of Texas at Austin, 10611 Exploration Way, Austin, Texas 78713-8924, USA

³ School of Earth Sciences, The Ohio State University, Columbus, 43210, USA

Abstract: The Devonian Donghe Sandstone complex in North Uplift of the Tarim Basin comprises of a series of diachronous sandy intervals deposited from the Late Devonian to Early Mississippian. They are constrained by a Late Devonian to Early Pennsylvanian 2nd-order supersequence and can be subdivided into five 3rd-order sequences, namely, S1, S2, S3, S4, and S5, from the oldest to youngest. Cores from four wells, 40 wireline logs, 410 thin sections, and porosity and permeability data from 639 spots from four wells were used to study the sediment provenance, build up the sequence-stratigraphic model of S5, and characterize the reservoirs at a feet scale. Detrital modes of sandstone from point counting indicate that Donghe Sandstone is directly sourced from recycled orogeny. The low content of feldspar and volcanic rock fragments suggests that Donghe Sandstone is recycled from sediment with a cratonic ultimate source. 1D and 2D chronostratigraphic correlation shows that at least 12 4th-order high-frequency sequences (HFSs), from the oldest HFS1 to the youngest HFS12, can be recognized in S5. Each HFS is characterized by a general trend of shallowing-upward facies assemblage. Sequence boundaries were defined at where regionally correlatable deep-water facies overlaying shallow-water facies. There is a general shallowing-upward trend in the S5 3rd-order sequence, characterized by a systematically increasing proportion of shallow-water facies (foreshore and upper shoreface), and a decreasing proportion of deep facies (offshore transition and lower shoreface). The shallowing-upward trend within both 3rd- and 4th-order sequences is resulted from a combined effect of eustatic sea-level change, tectonic activity, and sediment supply. The sequence-stratigraphic model of Donghe Sandstone S5 is similar to the rift-basin sequence-stratigraphic model. Sweet spots were defined as porosity >15% and permeability >100md intervals, and their distribution and lateral continuity were investigated. HFS is one of the primary controls on the distribution of sweet spots distribution and can be used to guide hydrocarbon exploration.

Key words: high-frequency sequences, shoreline systems, reservoir heterogeneity, Tarim Basin

1 Introduction

Marine clastic depositional systems are limited in China. The Donghe Sandstone is the first marine sandstone for hydrocarbon discovery in China. They are a series of thick marine siliciclastic intervals deposited in shoreline systems (Zhu Xiaomin et al., 2004; Zhang Huiliang et al., 2009), with very good production in the Tarim Basin, north west of China (Zhang Daquan et al.,

1991; Wang Zhaoming et al., 2004; Yin Nanxin et al., 2014). The study interval in this paper, Donghe Sandstone S5 is deposited during the Early Mississippian, which was an icehouse period. During an icehouse period, high frequency and high amplitude of eustatic change produces a juxtaposition of shallow facies, deep facies, and exposure (Frakes and Francis, 1988; Frakes et al., 1992). An icehouse period also produces frequent and long-distance shoreline transit (Blum and Hattier-Womack, 2009).

* Corresponding author. E-mail: ziyuan_wang579@126.com

Previous geological study on Donghe Sandstone mainly focused on the hydrocarbon migration (Luo et al., 2015) and depositional systems (Zhu Xiaomin et al., 2004; Zhang Huiliang et al., 2009). However, little has been published on the sediment provenance, high-resolution sequence stratigraphy, and fine-scale reservoir quality study of Donghe Sandstone.

Using sequence stratigraphy to understand hydrocarbon reservoir has been studied for long (Leckie and Walker, 1982; Cattaneo and Steel, 2003; Al-Ramadan et al., 2005; Zecchin, 2007; Jackson et al., 2009; Cheng Yongsheng, 2015; Xian Benzong et al., 2017). It is crucial to use high-resolution sequence stratigraphy in reservoir characterization because sequence stratigraphy can predict facies and grain size distribution in order to understand the reservoir heterogeneity (Zecchin, 2007; Guo Wei et al., 2015; Zecchin and Catuneanu, 2015; Lai Jin et al., 2016; Li Weiqiang et al., 2017; Mei Mingxiang and Liu Shaofeng, 2017; Sabbagh Bajestani Mahnaz et al., 2017; Zhang et al., 2017b). The fine-scaled reservoir is defined as reservoirs within high-frequency sequence scale (Zecchin and Catuneanu, 2015). This paper provides a detailed discussion on the sequence model of Donghe Sandstone S5 and the vertical distribution and lateral continuity of sweet spots. The relationship between HFS and distribution of sweet spots will be discussed. It will help us understand internal heterogeneity of siliciclastic-dominated shallow-marine reservoirs and how to use HFS to evaluate and even predict the distribution of good reservoirs, which will have significant implications for hydrocarbon exploration strategy of Donghe Sandstone in the Tarim Basin.

Densely distributed cores and wire-line logs are commonly used in the study of depositional systems and sequence stratigraphy (Carvajal and Steel, 2006; Fairbanks et al., 2016; Koo et al., 2016; Zhang et al., 2016; Liu et al., 2017; Zhang et al., 2017a; Liu et al., 2018; Zhang et al., 2018). This study uses densely distributed thin sections and porosity, permeability data, wire-line logs, and cores to characterize the sediment provenance and vertical and horizontal facies variations, which helps to answer the following questions on Donghe Sandstone: What is the tectonic setting of provenance terraces of Donghe Sandstone? What is the 4th-order sequence stratigraphic framework of Donghe Sandstone? What is (are) the driver (s) of Donghe Sandstone sequence? What are the similarities and differences of Donghe Sandstone sequence model and rift basin sequence model proposed by Martins-Neto and Catuneanu (2010)? What is the distribution of sweet spots in Donghe Sandstone? What is the relationship between the distribution of sweet spots and HFS in Donghe Sandstone?

2 Geological Setting

2.1 Study area and regional tectonic history

The Tarim Basin, located in the northwest of China (Fig. 1a), is an important hydrocarbon-producing basin. In this research, the study area is the Donghe Oil Field, which is located in the North Uplift northeast of the Tarim Basin (Fig. 1b).

The Tarim Basin is bounded by the Tianshan Mountains to the north, Kunlun Mountains to the southwest and Altyn Mountain to the southeast (Şengör et al., 1993; Xiao et al., 2010) (Fig. 1b). The relationship of the position of the Tarim Craton to other main terranes during Precambrian is unknown (Huang et al., 2005). The Tarim Basin plays an important role in the reconstruction of Rodinia and Pangea supercontinents (Rogers and Santosh, 2003). Tarim block has sedimentary rocks overlying a Precambrian basement (Tarim Craton), which formed in Archaean, Palaeoproterozoic, Mesoproterozoic and Neoproterozoic (Lu et al., 2008). Sedimentary rock overlying the Precambrian basement is a composite and stacked basin. During the Late Devonian when the Tarim Basin began to extend, the Paleo-Tethys Ocean flooded into the Tarim Basin from the west (Zhang Huiliang et al., 2009) (Fig. 3). Before the deposition of Donghe shoreline systems, two main uplifts—Central and North—were located in the middle and north of the Tarim Basin, respectively (Fig. 1b).

2.2 General stratigraphy

Donghe Sandstone intervals, mainly deposited in a 2nd-order sequence (Fig. 2), are composed of five sandy units (five shoreline systems), with the oldest system in the east and the youngest in the northeast of the Tarim Basin resulted from the topography of the basin and the marine-transgression direction (Figs. 1b, 2 and 3). These five shoreline systems formed five 3rd-order sequences. Figure 3 shows marine flooding stages during Late Devonian to early Carboniferous, each stage corresponding to each 3rd-order sequence of the Donghe shoreline system shown in Fig. 2. Notice the long distance shoreline transit in Fig. 3 is a typical depositional characteristic during icehouse period as proposed by Blum and Hattier-Womack (2009).

In this research, the study area is the Donghe oil field, which is located in the northeast of the Tarim Basin near the North Uplift (Fig. 1b). The study interval is S5 (marked in Fig. 2). We assume that the depositional rate is constant, and that the estimated duration of the study interval is about 5 Ma. A total of 12 Sequence boundaries within S5 were recognized so the average of each sequence is a 4th-order sequence with a duration of about

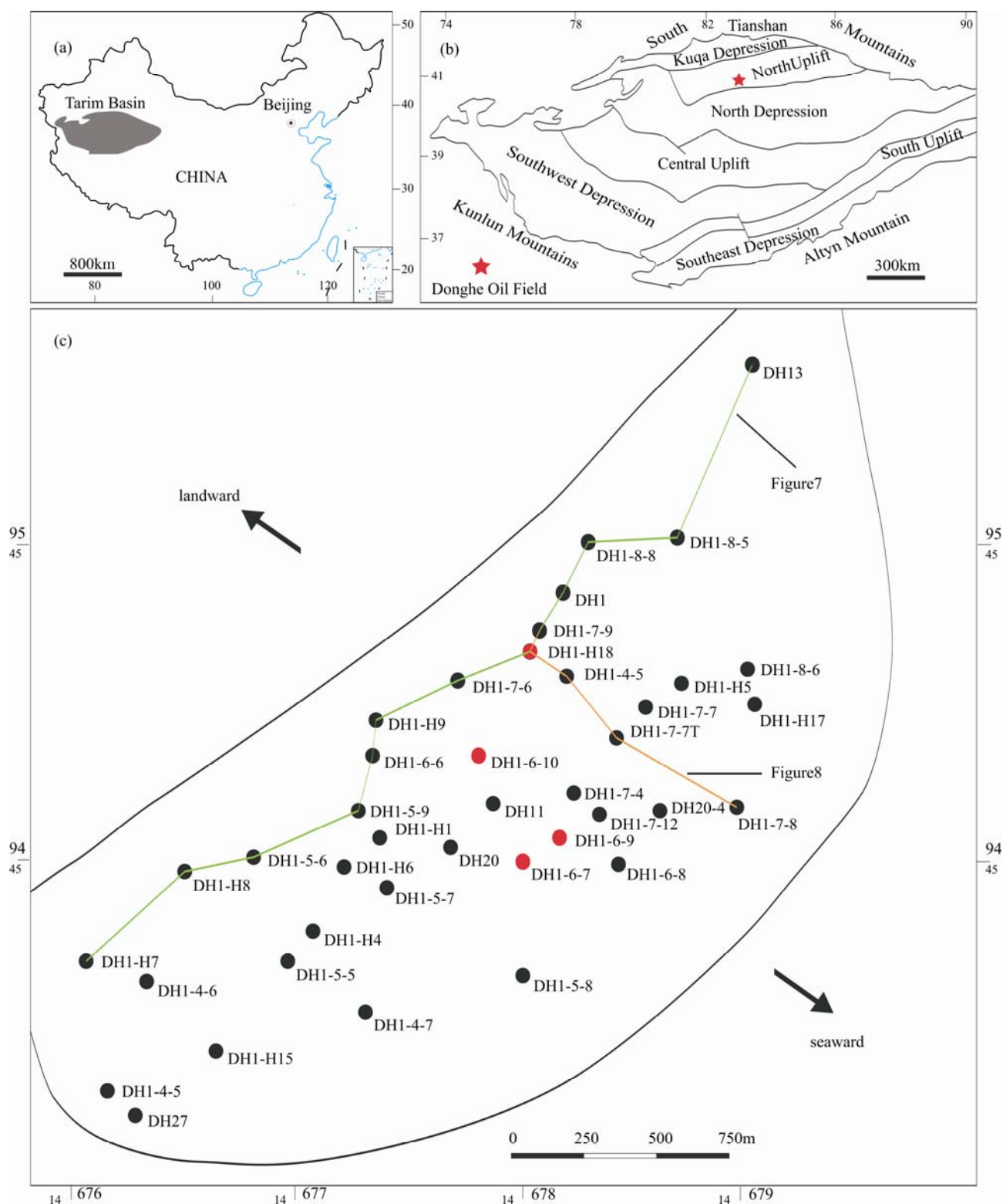


Fig. 1. Tectonic sketch map of the Tarim Basin.

(a), Location of the Tarim Basin. (b), structure map and location of study area (Donghe Oil Field) in the Tarim Basin. (c), well locations in the Donghe Oil Field. One depositional-strike cross-section (green) and one depositional-dip cross section (orange) are shown in Figs. 7 and 8, respectively. Four cored wells are shown in red. Figures 1a and b are modified from Guo Wei et al. (2015) (China basemap after China National Bureau of Surveying and Mapping Geographical Information).

400 kyr, which is the 4th-order Milankovitch eccentricity cycle (Hays et al., 1976). During the icehouse climate

regimes (the same as the climate when S5 is deposited), small-scale cycles (4th-order or lower rank) were referred

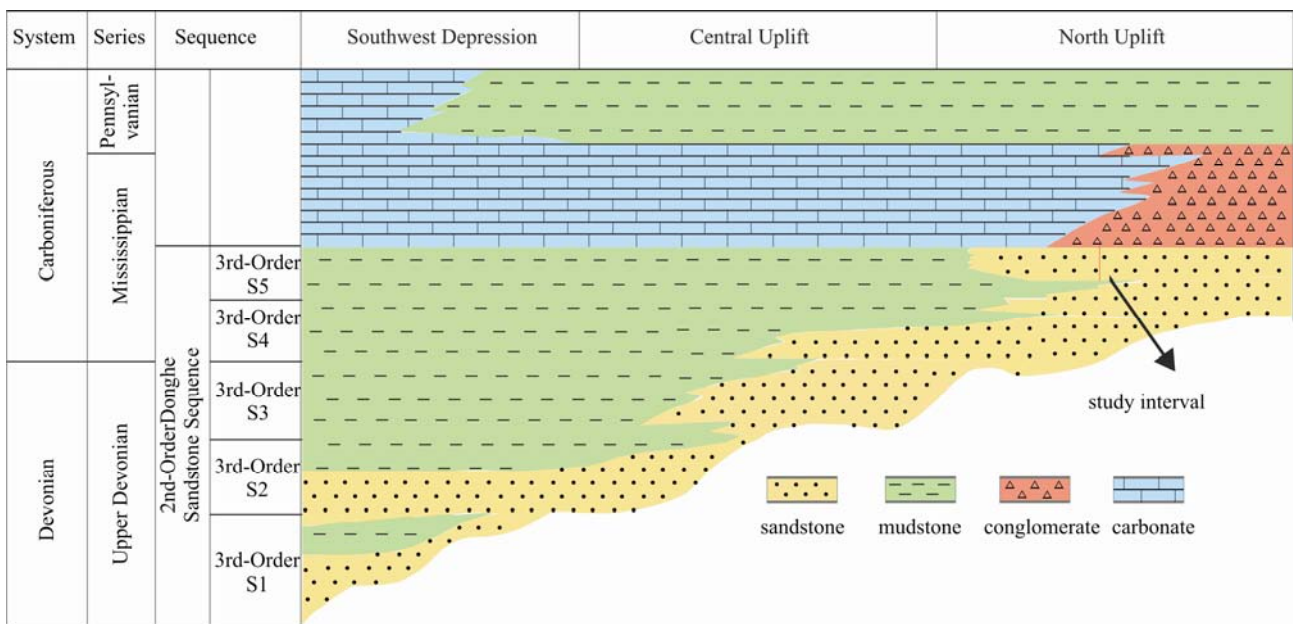


Fig. 2. General lithology characteristics of Southwest Depression, Central Uplift, and North Uplift during Late Devonian to Early Pennsylvanian in the Tarim Basin. Modified from Zhang Huiliang et al. (2009).

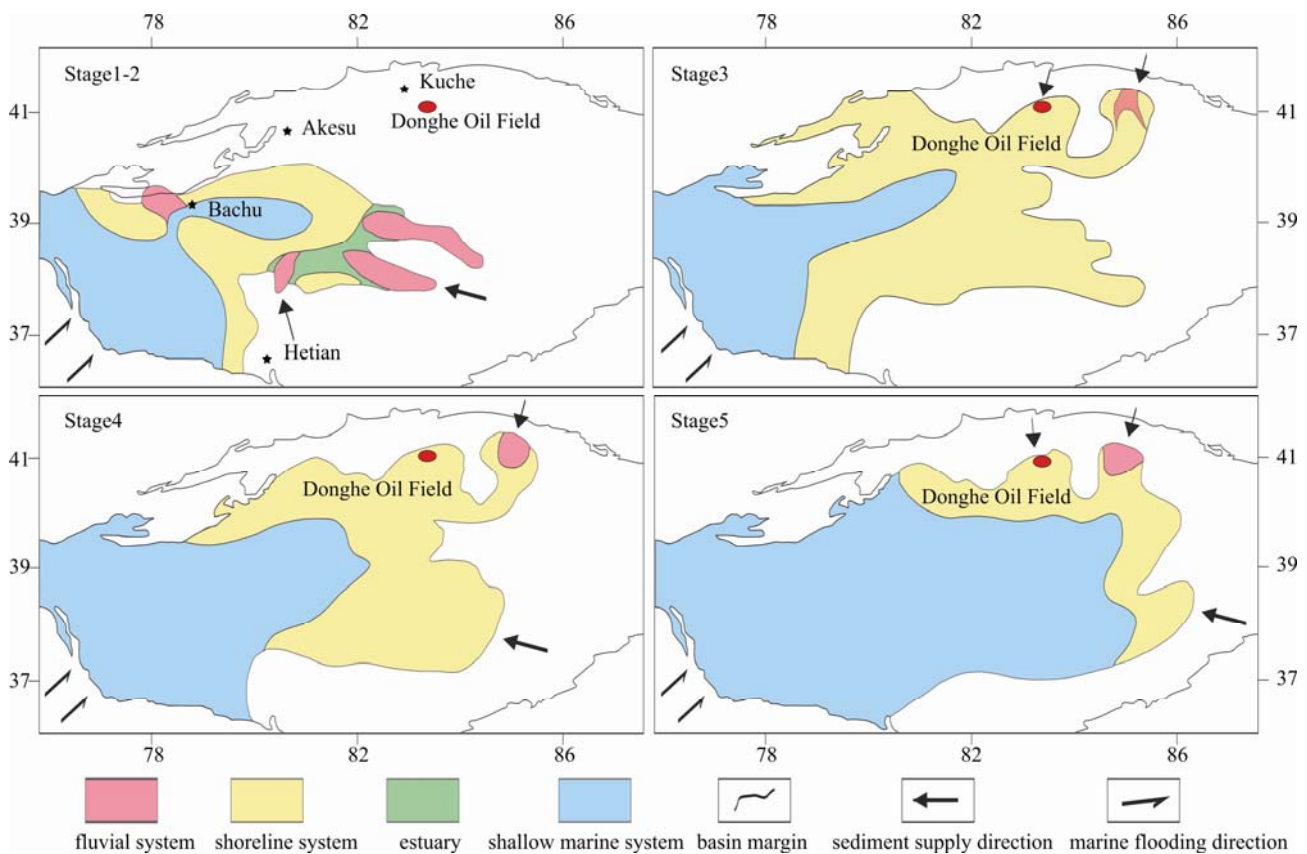


Fig. 3. Marine flooding stages during Late Devonian to early Carboniferous. Each stage is equal to each 3rd-order sequence of Donghe shoreline system shown in Fig. 2. Modified from Zhang Huiliang et al. (2009).

to as high frequency depositional sequences (Kidwell, 1997; Naish and Kamp, 1997). In order to avoid nomenclatural and methodological confusion, 4th-order sequence within S5 is called high-frequency sequence (HFS) in this paper as suggested by Catuneanu and

Zecchin (2013).

3 Samples and Methods and Data Set

Four densely-distributed continuous cores were

described: DH1-6-9, DH1-H18, DH1-6-10, and DH1-6-7. Lithology, bed thickness, grain size, vertical grain-size trend (fining or coarsening upward), and sedimentary structure were documented. Five facies were identified based on the core data, and these facies are foreshore, upper shoreface, lower shoreface, offshore transition, and alluvial fan. We analyzed 160 thin sections in four cored wells for grain size, mud content, and supplemental assistance for facies and sequence-boundary identification. Core description and thin sections were used to calibrate with well logs (gamma-ray). All thin-section samples were examined using transmitted-light microscopy under plane-polarized light and cross-polarized light. The thin sections were vacuum-impregnated with blue dye resin to highlight porosity. Photomicrographs were taken from 410 thin sections under microscope from DH1, DH1-6-6, DH1-6-8, DH1-6-9, DH1-H18, DH4-4, and DH13 well. The point counting was done using JMicroVision (1.2.7 version) and we make sure to count more than 300 grains (quartz, feldspar, and lithic fragment) in each thin section. A total of 639 core plugs were sampled every 0.12m (0.3ft) in average and routine core analysis was conducted at China National Petroleum Corporation Laboratories. Porosity and permeability were measured for each individual sample using helium ambient conditions and Darcy's Law, respectively. GR log from 40 wells were used to build the 2D sequence- stratigraphic model of S5. Finally, based on the facies assemblage from the core data and 2D sequence - stratigraphic model, detailed 1D high-frequency sequence-stratigraphic model is built by recognizing regional correlatable surfaces where deep facies overlay shallow facies.

4 Results

4.1 Detrital modes of sandstones

Different tectonic settings of provenance terraces are primary controls on detrital modes of sandstones, although other secondary factors will also affect sandstone composition. Some depositional processes may locally enhance stable fraction such as quartz and remove relatively unstable lithic grains and feldspars (Dickinson et al., 1983). Other secondary factors that change sandstone composition are relief, climate, transport mechanism, and diagenesis (Dickinson and Valloni, 1980; Maynard et al., 1982; Dickinson, 1985; Hessler et al., 2017). Studied sandstones are all sublitharenite with total quartzose grains 45%–91% (74% on average), feldspar grains 0–18% (4% on average), and polycrystalline lithic fragments 6%–38% (22% on average). The lithic fragments in Donghe Sandstone include sandstone-arenite, chert-arenite, and volcanarenite (Figs. 6c and d). QmFLt ternary diagram of

Fig. 4 shows fields for discrimination of sands derived from different types of provenances in continental blocks, magmatic arcs, and recycled orogens. In Fig. 4, most samples are plotted within quartzose recycled orogens.

4.2 Facies model

Based on core description for four wells and literatures (Zhang Huiliang et al., 2009; Zhu Xiaomin et al., 2004), Donghe Sandstone S5 is a shoreline system and mainly contains four facies: foreshore, upper shoreface, lower shoreface, and offshore transition. The other facies is conglomerate, overlying Donghe Sandstone S5. The boundary of the conglomerate facies and Donghe Sandstone can be easily recognized from both wireline logs and cores in the study area. The conglomerate facies, which is the proximal part of the alluvial fan deposit, abruptly overlays the Donghe Sandstone S5, and can be regionally correlated in the study area.

Foreshore, the part of the zone between average low tide and average high tide, has high hydrodynamic force. Grains are mainly fine-grained sand (Fig. 6a). Swash cross bedding and parallel bedding are common (Fig. 5b). In the upper part of S5, the foreshore facies usually exists at the top of each HFS. Shoreface, the part of the zone between average low tide and wave base, can be subdivided into upper shoreface and lower shoreface. In the upper shoreface, hydrodynamic force is high and grain size is coarser. Medium- to fine-grained sandstones are the main

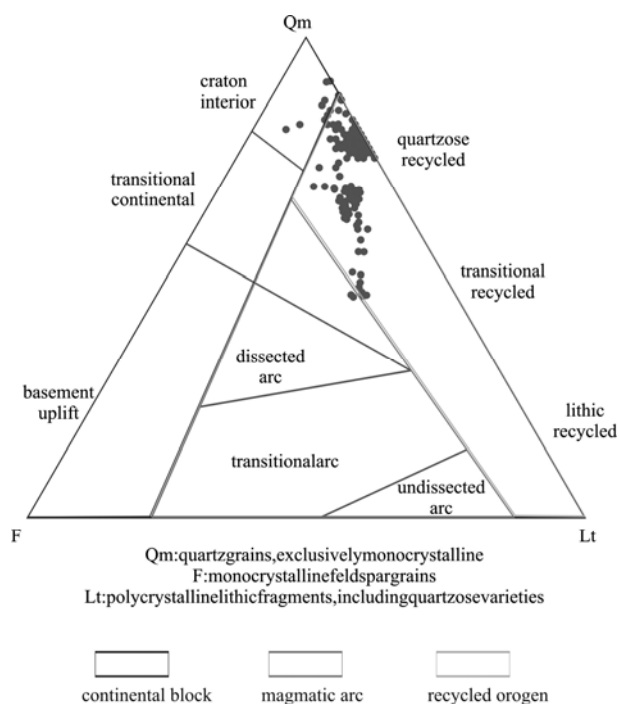


Fig. 4. Detrital compositions and classification of Donghe Sandstone in provenance-discrimination diagrams. Tectonic setting classification from Dickinson et al. (1983).

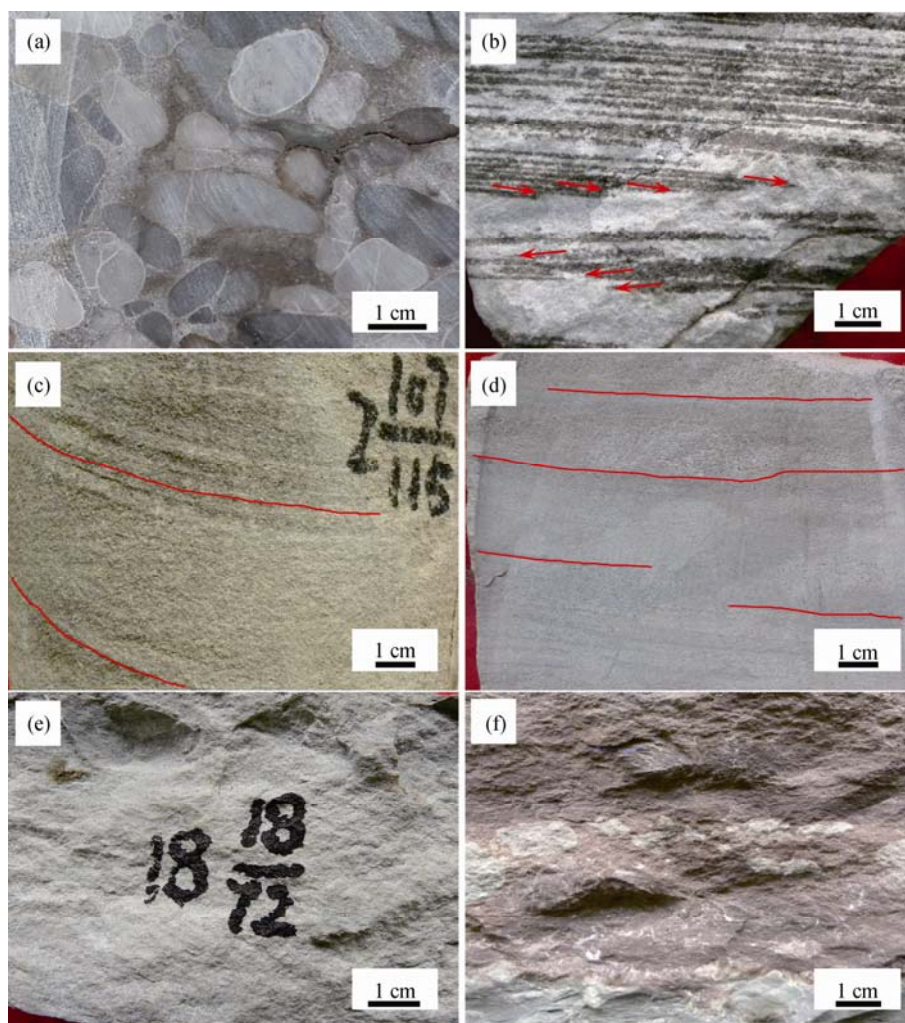


Fig. 5. Donghe Sandstone S5 cores.

(a), Conglomerate, proximal part of alluvial fan deposit; DH 1-6-9. (b), Fine-grained sandstone, with wave-swash cross-bedding, arrows are deduced paleocurrent direction; foreshore deposit; DH 1-6-9. (c), Medium-grained sandstone (oil-stained), with trough cross-bedding; some highlighted by red lines; upper shoreface deposit; DH1-6-7. (d), Laminated muddy siltstone, horizontal bedding; some gray-muddy strips highlighted by red lines; lower shoreface deposit; DH1-6-6. (e), Muddy siltstone; offshore transition deposit; DH1-H18. (f), Silty mudstone; offshore transition deposit; DH1-H18.

deposit (Figs. 6c and d). Trough, tabular, and parallel cross-bedding can be observed (Fig. 5c). In the lower shoreface, energy is low and siltstone is common (Fig. 6b). In the lower part of the lower shoreface, grain size is finer and mud content is higher; laminated muddy siltstone is dominant (Fig. 5d). In the upper part of the lower shoreface, grain size is larger; siltstone is dominant and mud is absent. Offshore transition is below the storm wave base, with low depositional energy. Mudstone, silty mudstone (Fig. 5f), and muddy siltstone (Fig. 5e) are dominant, and planar cross-bedding is common.

4.3 2D Sequence-stratigraphic framework

In this study, the building blocks of 2D sequence is defined as flooding surface-bounded sequences (Galloway, 1989) or clinothems (Rich, 1951) in order to

subdivide Donghe Sandstone stratigraphy. These flooding surface-bounded sequences are expressed by high gamma ray value in the GR logs. This method for sequence division is widely used in the sequence stratigraphic study of shoreline depositional systems (Carvajal and Steel, 2006; Zhang et al., 2016).

These flooding surface-bounded sequences are expressed by high gamma ray value in the GR logs. The 2D sequence-stratigraphic framework is established by correlating GR logs in three depositional-strike cross-sections and nine depositional-dip cross-sections, with some cross-sections shown in Fig. 1. Seaward is southeast and landward is northwest. The 2D sequence-stratigraphic model has been calibrated with the 1D model (introduced in Section 4.4) to make sure sequence boundaries in the latter are regionally correlatable. One depositional-strike

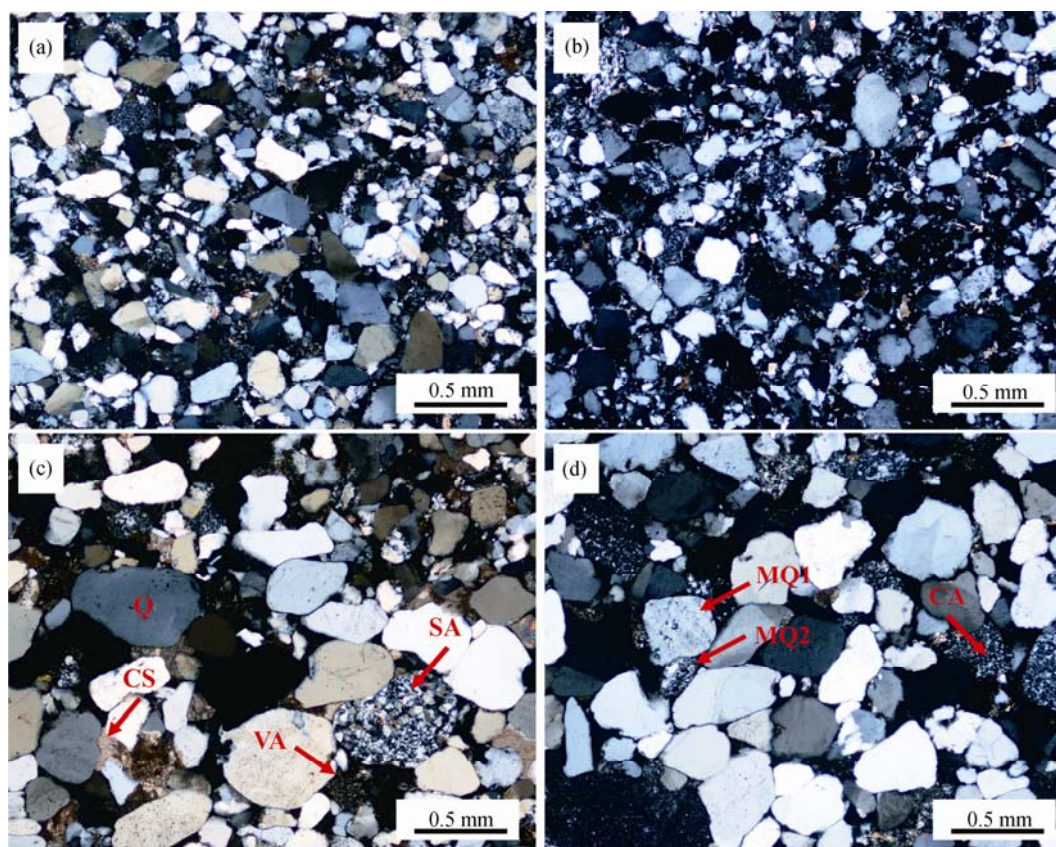


Fig. 6. Thin sections of Donghe sandstone S5.

(a), Fine sandstone: submaturesubliarenite, foreshore deposit. (b), Fine sandstone: submaturesubliarenite, lower shoreface deposit. (c), Medium sandstone: mature subliarenite, upper shoreface deposit. (d), Medium sandstone: mature litharenite, upper shoreface deposit. All thin sections are from DH1-H18 well and are under cross-polarized light. Notice evidence of metamorphism from distinctive inclusions (MQ1) and characteristic polycrystallinity (MQ2). Abbreviations: Q, Quartz; MQ, Metamorphic quartz; CS, Calcite cement; SA, Sandstone-arenite; CA, Chert-arenite; VA, Volcarenite. Sandstone classification based on Folk (1980).

cross-section and one depositional-dip cross-section are shown in Figs. 7 and 8, respectively. Each cycle boundary is regionally correlatable; some spikes that cannot be regionally correlated are interpreted as autogenic in origin. Shoreline trajectory is defined as the path of shoreline migration and has been considered to be a function of the rate of generation or decreasing of accommodation space, by sea level change and tectonism, and the rate of sediment supply (Muto and Steel, 2002). In Fig. 8, shoreline edges were identified in each high frequency sequence and were connected for shoreline trajectory. Figure 8 clearly shows a progradational stacking pattern from HFS2 to HFS5 and a near-aggradational stacking pattern from HFS6 to HFS11. For all wireline logs, tops are flattened at the base of conglomerate facies.

4.4 1D High-frequency sequence-stratigraphic framework

In this study, the sequence boundary of 1D high-frequency sequence is also defined as flooding surface with high gamma values (Galloway, 1989). Within each high-frequency sequence, five facies were identified including four facies from shoreline system: foreshore,

upper shoreface, lower shoreface, and offshore transition, and one facies from alluvial fan system: conglomerate facies. Conglomerate facies can be correlated effectively with all wells in the study area and its bottom is flattened for well correlations (Figs. 7 and 8). Facies were identified based on lithology, grain size, sedimentary structures, logging response, literatures (Zhu Xiaomin et al., 2004) and supported by the long-term trend of the lower frequency 3rd-order S5 sequence (Fig. 9b). Using lower frequency sequence to predict the architecture and facies assemblage of higher-frequency cycles is proposed by Cross (1988) and Swift et al. (1991) although Zecchin (2007) suggested that this predicting cannot be used in the place where local factors exert a dominant control on the architecture of deposit.

Within each high-frequency sequence, there is a shallowing-upward trend of facies assemblage. Foreshore is the shallowest facies, with a moderate to high gamma value, and the wave-swash cross-bedding is common. Upper shoreface is shallower than lower shoreface; it has the sandiest facies and lowest gamma value and trough-cross stratified sandstone can be observed. Lower

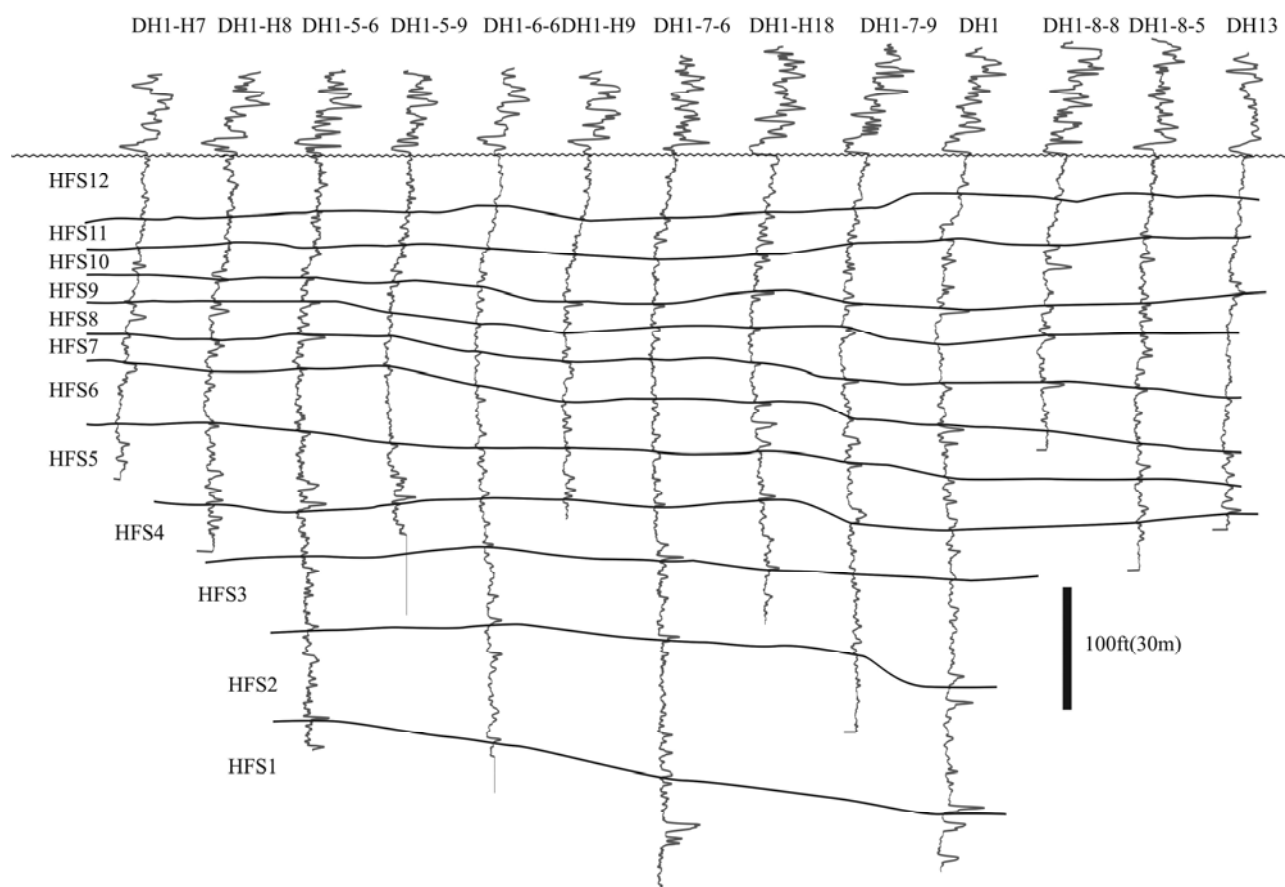


Fig. 7. 2D sequence-stratigraphic model in a depositional-strike cross-section based on GR logs. For each well, from left to right, GR value increases from low to high. See Fig. 1 for line location.

shoreface is shallower and sandier than offshore transition, and muddier than upper shoreface; it has a moderate gamma value. Sometimes the wave ripple beds and contorted bed can be seen (Coe, 2003). Offshore transition is the deepest facies and most muddy, and it has the highest gamma value. Some burrowed silty mudstones can be observed (Coe, 2003). Cycle top is recognized where shallower facies are abruptly capped by relative deeper facies and should be regionally correlatable (Mitchum and Van Wagoner, 1991).

The 1D high-frequency sequence-stratigraphic framework is established by two cored well DH1-H18 and DH1. DH1 well has the most completed wireline logs through which we can see all facies assemblages. Well locations are labeled in Fig. 1c. Donghe Sandstone S5 is a 3rd-order shallowing-upward sequence composed of at least 12 (labeled HFS1 to HFS12 in the DH1 well, Fig. 7) 4th-order HFS (cycles) (Fig. 7).

4.5 Reservoir quality

The DH1 well is selected to study the relationship between facies and reservoir quality. The porosity and permeability of ninety-five core plugs were obtained from

foreshore, upper shoreface, lower shoreface, and offshore transition zone facies in the DH1 well. Those data were plotted in Fig. 10. The average of porosity and permeability of all core plugs is summarized in Table 1. From Fig. 10 and Table 1, Upper shoreface and lower shoreface have slightly higher porosity compared with foreshore and offshore transition zone. However, there is a significant permeability difference between different facies. Upper shoreface has the highest permeability although the values vary from less than 1 md to more than 1000 md. Most of the permeability data from upper shoreface are distributed from 10 md to 1000 md. Foreshore and lower shoreface have lower permeability compared with upper shoreface. Main permeability values range from 1 md to 40 md. The offshore transition zone has the lowest permeability with data ranging from 1md to 10 md.

Table 1 Summary of reservoir quality data in each facies of DH1 well

Facies	Porosity (%)	Permeability (md)
Foreshore	11.9	16.7
Upper shoreface	15.3	103.2
Lower shoreface	14.2	7.9
Offshore transition	13.1	2.2

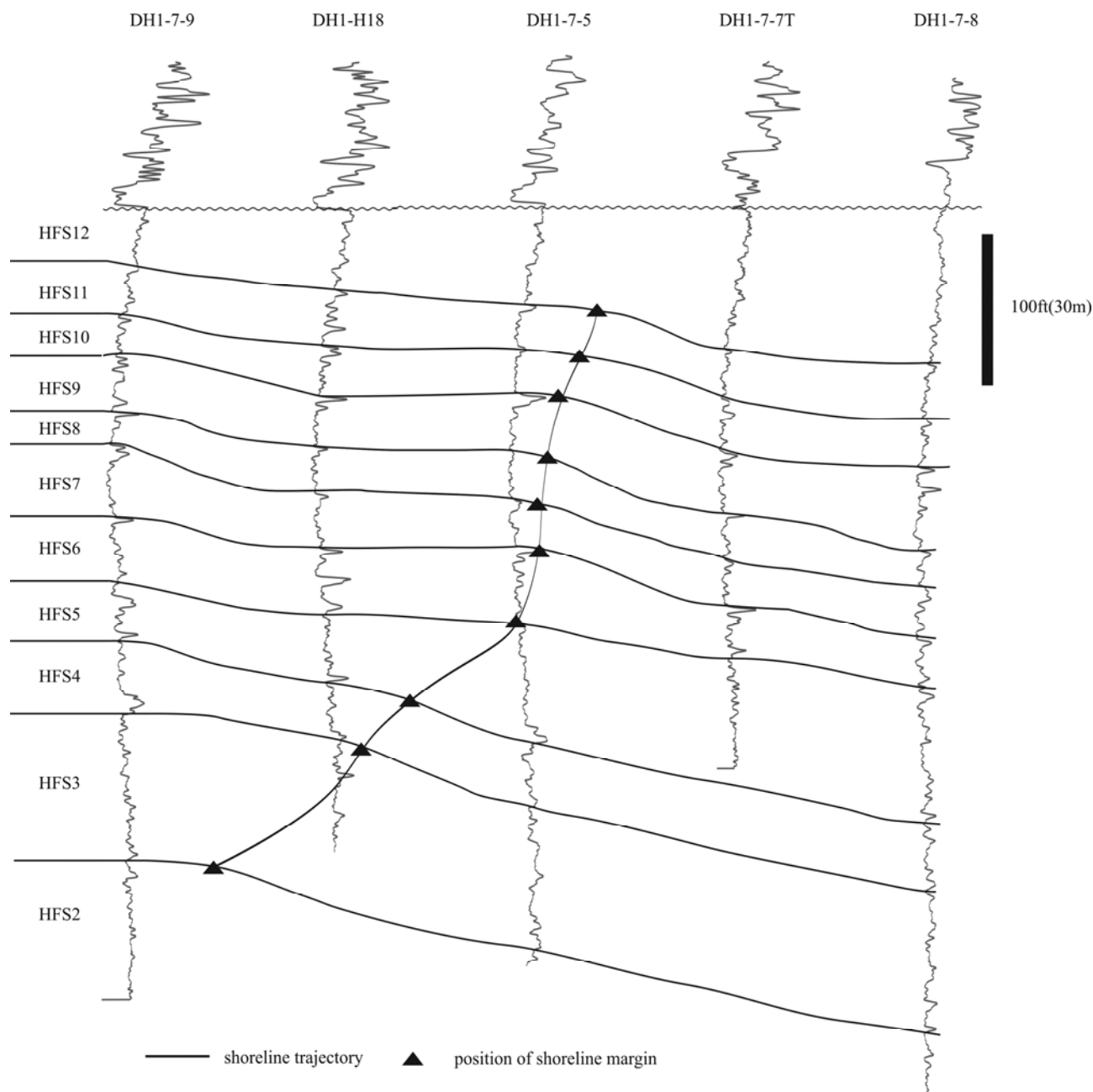


Fig. 8. 2D sequence-stratigraphic model in a depositional-dip cross-section. For each well, from left to right, GR value increases from low to high. See Fig. 1 for line location.

The Primary aim of hydrocarbon exploration is to find the sweet spots. In this study, the close spaced sampling interval of core plug (sampled every 0.12m) provides an excellent opportunity to characterize the Donghe Sandstone reservoirs. We define the sweet spots as intervals with porosity >15% and permeability >100md (Fig. 11). Tentative correlation of sweet spots was made among DH1 well, DH6-9 well, and DH11 well to investigate the lateral continuity of sweet spots and the controls on the sweet spot distribution. There are a total of fourteen sweet spots defined in DH6-9 from HFS6 to HFS 12, and six of them can tentatively correlate with sweet

spots in both DH1 and DH11 well. Five of them can be tentatively correlated with sweet spots in either DH1 or DH11 well. HFS6 to HFS12 is characterized by foreshore in the upper part of each HFS and upper shoreface in the lower part of each HFS (Fig. 9b).

5 Discussions

5.1 Sediment provenance

Orogenic recycling occurs in tectonic settings such as subduction complex, back-arc thrust belts, and suture belts (Dickinson and Suczek, 1979; Dickinson, 1985).

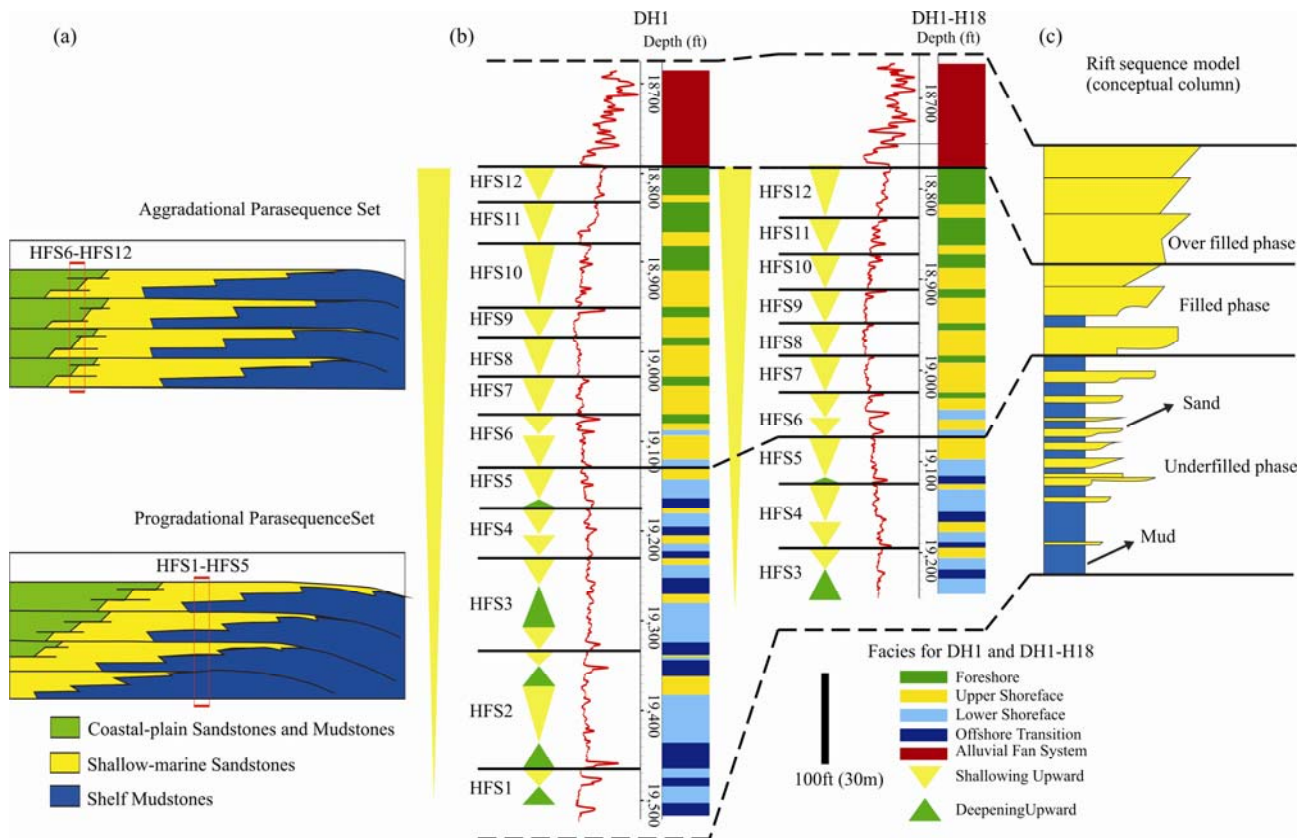


Fig. 9. Comparison of facies stacking pattern of Donghe sandstone with classic geological models. (a), progradational and aggradational stacking patterns from Van Wagoner et al. (1990), the similar facies assemblages with HFSs of Donghe Sandstone S5 are indicated in red boxes. (b), 1D sequence-stratigraphic model of Donghe Sandstone S5 and correlation with conceptual column of rift sequence model to right. Top and bottom of sequence in DH1 and DH1-H18 well are marked with dashed line because entire sequence is not completely cored. (c), conceptual column of rift sequence model from Martins-Neto and Catuneanu (2010).

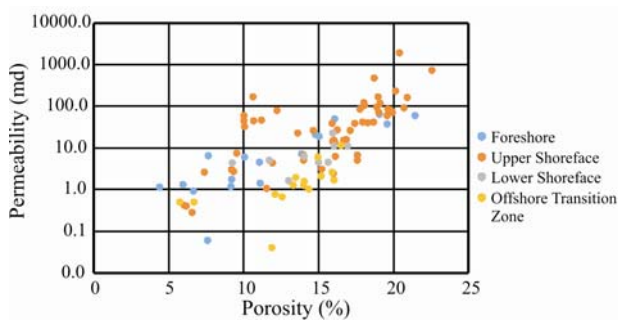


Fig. 10. Porosity and permeability cross plot of four facies of Donghe sandstone S5.

Sandstone sourced from such provenances generally contains low feldspar content because igneous rocks such as granite which is rich in feldspar are not the primary source. Because of the abundant sandstone-arenite, chert-arenite, and volcanite in Donghe Sandstone, the sediment source is mainly sedimentary strata and subordinate volcanic rocks, exposed to be eroded by orogenic uplift of thrust sheet and fold belts (Dickinson et al., 1983). Based on seismic interpretation of regional distributed faults (Jia et al., 1998), tectonism is active

during the Paleozoic in the North Uplift of the Tarim Basin region. Furthermore, high content of quartz and low content of feldspar and volcanic rock fragments in Fig. 4 suggest that Donghe Sandstone is recycled from sediment whose ultimate source was cratonic, consistent with the idea that the Precambrian basement (Tarim Craton) has been uplifted and eroded with evidence of U-Pb detrital zircon data (Guo et al., 2005; Zhang Huiliang et al., 2009; Shu et al., 2011). Recycling of quartzose sands such as those of the Donghe Sandstone typically involves deformation and uplift of miogeoclinal successions (Dickinson et al., 1983). A miogeocline is an area of sedimentation that occurs in an extensional tectonism and in which shallow-water clastic systems are dominant—consistent with the extensional tectonic history of the Tarim Basin and depositional systems of Donghe Sandstone shown in Fig. 3. The relationship between tectonism and the sequence-stratigraphic framework of DongheS5 will be discussed in detail in Section 5.4.

5.2 S5 sequence-stratigraphic model

Based on the classification from Zecchin (2007), shoreface HFSs can be divided into three main categories:

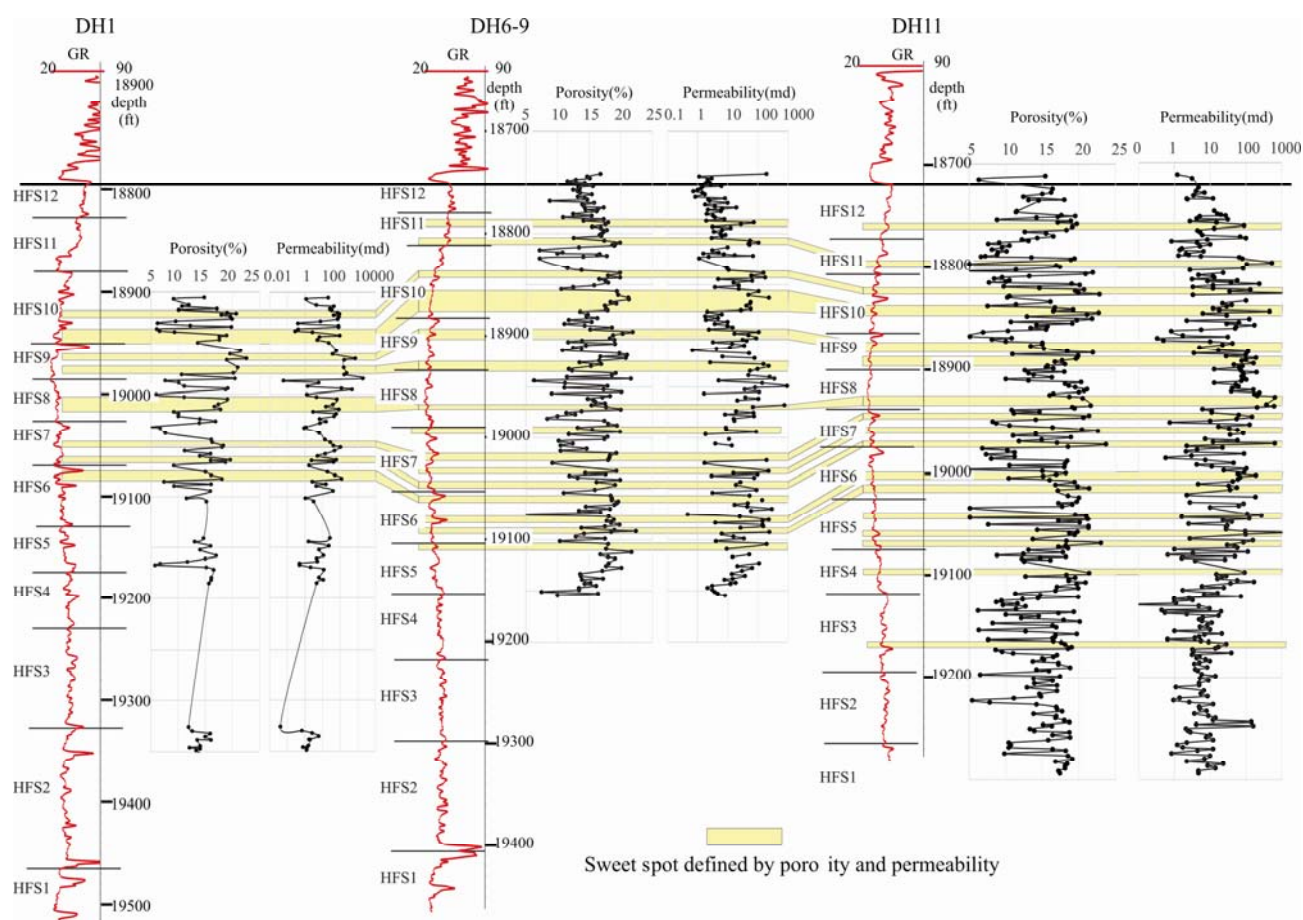


Fig. 11. Sweet spots distribution and tentative correlation in DH1, DH6-9, and DH11 wells.

R cycles, with a dominant regressive interval; T-R cycles, with transgressive and regressive intervals of similar thickness; T cycles, showing a dominant transgressive interval. In Fig. 9b, R cycles dominant the study interval, and only HFS3 is T cycle and HFS1 is T-R cycle. From HFS1 to HFS4, cycle tops are overlaid by offshore transitions. The cycle top of HFS5 is capped by lower shoreface. The facies assemblage of HFS1 to HFS5 is similar to (not correlated to) that in the progradational stacking pattern shown in Fig. 9a (indicated by the red box), which is supported by shoreline trajectory in Fig. 8. The cycle tops of HFS6 to HFS11 are the upper shoreface overlying foreshore. HFS12 is capped by an alluvial-fan conglomerate deposit, indicating that no marine accommodation space existed. The facies assemblage of HFS6 to HFS12 is similar to (not correlated to) that in the aggradational stacking pattern shown in Fig. 9a (indicated by the red box), which is supported by shoreline trajectory in Fig. 8. From HFS1 to HFS12 to conglomerate facies, there is a decreased proportion of deep facies and an increased proportion of shallow facies. Facies changed dramatically from marine offshore transition to terrestrial-

conglomerate (alluvial-fan) facies, suggesting the systematic decrease of accommodation space and/or increase of sediment supply.

There are some similarities between the Donghe Sandstone S5 sequence-stratigraphic framework and the rift-basin sequence model proposed by Martins-Neto and Catuneanu (2010). Tentative correlation of Donghe Sandstone S5 with the rift-basin sequence model is shown in Figs. 9b and c. HFS1 to HFS5 relative muddy cycles stand for the unfilled phase formed when the ancient Tethys Sea was still extending and sediment did not fill the accommodation created by extension tectonism, which is further supported by the deepening upward facies assemblage and existence of T cycle and T-R cycle (Fig. 9b). HFS6 to HFS12 sandy upper shoreface and foreshore is the filled phase, suggesting ceased tectonic subsidence and corresponding marine transgression, and gradual filling of accommodation, evidenced by the lack of deepening upward facies assemblage and dominant R cycles from HFS6 to HFS12 (Fig. 9b). Conglomerate facies from alluvial fan is the overfilled facies, indicating that accommodation space is totally consumed by

sediment supply. The general shallowing-upward facies assemblage in Fig. 9b is consistent with the rift-basin sequence model (Fig. 9c) proposed by Martins-Neto and Catuneanu (2010).

Based on the 1D high-frequency sequence-stratigraphic framework of S5, we suggest to make revisions on the rift-basin sequence model proposed by Martins-Neto and Catuneanu (2010). Conceptual model should show a shallowing-upward facies assemblage (Fig. 9b) but not just a coarsening-upward grain size change (Fig. 9c) because in some circumstance grain size is not always larger when the water depth become shallower (see HFS6 to HFS12 in Fig. 9b and red box in Fig. 9a). Size of grain in coastal-plain mudstone is definitely smaller than that in shallow marine sandstone (Fig. 9a). Size of grains in foreshore is smaller than that in upper shoreface because of weaker hydrodynamic forcing (Fig. 9b).

5.3 Autogenic and allogenic processes

Factors that are external to the depositional system are called allogenic processes, such as climate, eustasy, tectonics, and sediment supply (Einsele et al., 1991). Autogenic processes are those internal to the depositional system (Einsele et al., 1991) such as delta lobe switching (Pulham, 1989) and 'autoretreat' process (Muto and Steel, 1997; Muto and Steel, 2002). At the scale of 4th-order and lower rank cycles, both allogenic and autogenic processes can form the sequence boundary. However, only the autogenic processes that can influence the direction of shoreline shift play a role in the formation of sequence stratigraphic surface (Catuneanu and Zecchin, 2013). A study of the Cisco Group—a reciprocal carbonate and clastic system in the Permian Basin, West Texas—suggests that autogenic processes caused local variations of cycle character while allogenic processes controlled regional systematic changes in cycle abundance, continuity, type, magnitude, and thickness (Yang et al., 1998). Sequence stratigraphy focuses on stratal stacking patterns, which are controlled by sediment supply and accommodation space, which in turn are mainly controlled by allogenic processes (Posamentier and Allen, 1999; Catuneanu et al., 2009; Zhang et al., 2018). Accommodation space is affected by tectonism and/or eustatic sea-level change. Syvitski and Milliman (2007) proposed the BQART model to quantify sediment supply. In this model, sediment discharge is mainly controlled by mean water discharge, drainage area, maximum relief, and basin average temperature. Maximum relief and drainage area are ultimately controlled by tectonism.

The most common and possible autogenic process in Donghe S5 is lobe switching. The most detailed modern deltaic lobe switching comes from the Mississippi deltas.

Coleman (1988) pointed out that the Mississippi system switches the locus of deltaic deposition on average every 1500 years although autogenic processes could affect time scale up to 105 yrs (Muto and Steel, 2002; Amorosi et al., 2005; Stefani and Vincenzi, 2005). The average of HFS duration of DongheS5 is about 400kyr, which is much longer than the lobe switching period of Mississippi deltas, suggesting that lobe switching is not crucial on the development of HFSs of DongheS5.

Figures 7 and 8 show 11 regional correlatable surfaces that are probably controlled by allogenic processes. From the analogy of Upper Cretaceous outcrops in the Book Cliffs of east-central Utah studied by Hampson (2016), some uncorrelatable muddy spikes in HFS2 to HFS6 probably records autogenic switching of lobes during a short temporal scale. These intervals, which result from autogenic processes, are disregarded in order to simplify the building of sequence-stratigraphic framework of S5. However, for the scale like S5, some autogenic processes such as shoreline retreat could be the dominant driver of parasequence stacking patterns (Muto and Steel, 2002; Hampson, 2016). The formation of some HFSs of DongheS5 may be controlled by a mixture of internal and external factors. However, the relative contribution is hard or impossible to quantify and the discrimination between allo- and autogenic processes is just interpretation and tentative at best in many cases (Catuneanu and Zecchin, 2013). In general, the stacking patterns within DongheS5 are probably mainly controlled by orogenic activities with linked sediment supply in northern Tarim Basin.

5.4 Sequence drivers

Zecchin (2007) proposed some factors that control the architecture of HFSs, and these factor are crucial to reconstruct the depositional history. Factors which may be related to the S5 include: 1) the interplay between the rate of accommodation development and the rate of sediment supply (A/S); 2) the amplitude and shape of the relative sea-level curve.

The Donghe Sandstone was deposited within a 2nd-order supersequence during extension of the ancient Tethys Sea in the Tarim Basin from Late Devonian to early Carboniferous (Zhang Huiliang et al., 2009). The Donghe Sandstone can be subdivided into five 3rd order sequences (S1, S2, S3, S4, S5) with each sequence a duration of approximately 5Ma. Based on the geographical mapping of different depositional systems (Fig. 3) in the different stages (S1 to S5) during late Devonian to early Carboniferous and vertical facies stacking pattern of S5 unit, we deduce that the stacking pattern and sequence-stratigraphic framework of Donghe Sandstone S5 is similar to the rift-basin sequence model

proposed by Martins-Neto and Catuneanu (2010). Tectonism is a dominant driver in controlling accommodation space in tectonically active basins such as rift basins (Martins-Neto and Catuneanu, 2010). We can see a typical shallowing-upward sequence of S5 in Fig. 9, as well as the systematic proportion of deep-facies decreases and shallow-facies increases within each HFS from the bottom to the top of DH1 and DH1-H18 wells. This shallowing-upward characteristics of S5 is consistent with the rift basin sequence model proposed by Martins-Neto and Catuneanu (2010).

Detrital modes of sandstone from point counting indicate that Donghe Sandstone is directly sourced from recycled orogeny. Low content of feldspar and volcanic rock fragments suggests that Donghe Sandstone is recycled from sediment with a cratonic ultimate source. Recycling of quartzose sands such as those of the Donghe Sandstone typically involves deformation and uplift of miogeoclinal successions (Dickinson et al., 1983). Tectonism especially the orogenic activities near north Tarim Basin proposed by Jia et al. (1998) played an important role in the sequence within S5. The sediment-supply probably increased significantly from HFS6 to HFS12 because the almost aggradational stacking pattern (Fig. 8) is thought to be a result of increasing sediment supply which is proposed by Swenson and Muto (2007) based on the mathematical modeling and flume experiment. The interplay between tectonism and eustasy has been detailed discussed (Zecchin et al., 2012; Zecchin et al., 2016). Based on detrital modes of sandstone, aggradational stacking pattern (Fig. 8), and regional orogenic activities in north Tarim Basin during Devonian and Carboniferous (Jia et al., 1998), orogeny and linked increasing sediment supply is the probable main driver of the S5 sequence of Donghe Sandstone. The study of upper Paleocene-lower Eocene Wilcox group in Gulf of Mexico also shows that shoreline transits of Wilcox group were caused by the variation of sediment discharge (Zhang et al., 2016). The frequency of Wilcox shoreline migration is in the scale of a few hundred thousand years, suggesting that the sediment supply can be the main driver of high frequency sequences.

Sea level may act as a secondary control of the 4th-order HFSs from HFS1 to HFS12, as evidenced by a flooding event at the bottom of each HFS. Figure 8 shows no sudden shift of shoreline-margin position; and the facies change in Fig. 9 is gradational but not dramatic, indicating that the amplitude of sea-level change is low and thus sea level is not a primary driver of S5. From HFS1 to HFS5, the eustatic sea-level rise can approximately balance the accommodation space lost by tectonism and sediment supply. However, because

tectonism and related sediment supply increased dramatically from HFS6, accommodation space is consumed significantly and the slowly rising sea level cannot make up the accommodation loss. At the end, the deposition of the Donghe shoreline system ceased when accommodation decreased to zero, and high relief in the drainage area resulted in the large supply of alluvial fan system overlying the top of S5.

Although based on the tectonic history of the North Uplift of Tarim Basin, orogeny and linked sediment supply controls are probably main drivers of stacking patterns of cycles in S5, one autogenic process called autoretreat proposed by Muto and Steel (2002) can be an alternative main drivers of S5. Autoretreat happened because the area of the clinoform surface of the delta must increase as a result of sea level rise and it is possible that the sediment supply will be inadequate to sustain progradation. The shoreline trajectory is thus characterized by a concave-landward shape (Muto and Steel, 2002). Autoretreat is a possible explanation of sequence drivers because of the extension of Tethys Sea with linked relative sea level rise (Fig. 3) and concave-landward shape of shoreline trajectory (Fig. 8).

5.5 Distribution of sweet spots and its controlling factor

Depositional facies exerted an essential control on the quality reservoirs in the Tarim Basin and elsewhere (dos Anjos et al., 2000; Zhang et al., 2008; Aminul Islam, 2009; Ajdukiewicz and Lander, 2010). Before the burial of sediment, different grain size and sorting in different facies controls the initial porosity and permeability. After the burial, different mineral composition in each facies have significant different response to mechanical compactions. For example, the quartz rich facies is resist to the early stage of mechanical compactions than clay rich facies and thus can preserve more initial porosities (Tobin and Schwarzer, 2014). Offshore transition zone contains abundant of ductile component such as clay minerals which is more easily to be compacted.

Average of permeability in upper shoreface is significantly higher than other facies. There are two reasons that upper shoreface has the best reservoir qualities. First, before burial, upper shoreface has larger grain size and better sorting compared with offshore transition zone. The size and sorting of the detrital grain assemblage is a major control on permeability, but not primary porosity. Second, more ductile minerals in offshore transition zone makes this facies susceptible to mechanical compaction. The mud-rich intervals in offshore transition zone, although not highly-developed, can be compacted easily and block the pore throat,

reducing the permeability significantly. It can be concluded that the upper shoreface is the most desirable exploration and exploitation facies in Donghe Sandstone.

It is obvious that the sweet spots are more likely to distribute in the lower part of each HFS (Fig. 11). The lower part of each HFS is dominated by upper shoreface deposit. If the tentative correlation is reliable, most of the sweet spots in Donghe Sandstone HFS6 to HFS12 are laterally connected. Because of the lack of data from HFS1 to HFS5 in DH1 well and DH6-9 well, the lateral continuity of sweet spots from HFS1 to HFS5 cannot be determined. However, the concentration of sweet spots from HFS1 to HFS5 is much lower than that of HFS6 to HFS12, probably because of the dominant lower shoreface and offshore transition deposit (Fig. 9). Zecchin and Catuneanu (2015) mentioned that HFS controls the facies stacking patterns. Furthermore, in this case, facies controlled grain size, sorting, and the distribution of brittle mineral (quartz and feldspar) and ductile mineral (most clay minerals, mica) deposit. The grain size and sorting of the detrital grain assemblage control on initial permeability, and the brittle and ductile mineral deposit react significantly different to compaction so the consequent reservoir quality varies a lot. Thus HFS is one of the primary controls on reservoir quality. This progressive relationship is excellently expressed in Fig. 11. HFS6 to HFS12 controlled the dominant of foreshore and upper shoreface. Within each HFS, foreshore overlays the upper shoreface. The upper shoreface has higher porosity and permeability because of the coarser grains and better sorting compared with other facies. Thus the sweet spots are normally in the lower part of HFS6 to HFS12. The study of HFS is essential to the evaluation, prediction of the reservoir quality and characterization of lateral and vertical heterogeneity. Defining the HFS is a great help in locating sweet spots for oil and gas exploration.

6 Conclusions

(1) Donghe Sandstone S5 is a shoreline system that primarily contains four facies: foreshore, upper shoreface, lower shoreface, and offshore transition. S5 is overlaid by conglomerate facies from an alluvial fan system. Donghe Sandstone S5 is a 3rd-order shallowing-upward sequence deposited at the end of Tethys extension and related marine transgression. It can be subdivided into 12 HFSs with each HFS a duration of about 400kyr. The sequence-stratigraphic model of Donghe Sandstone is similar to the rift-basin sequence model proposed by Martins-Neto and Catuneanu (2010). The proportion of shallow-water facies increases and deeper-water facies decreases systematically

in each HFS from the bottom to the top of S5. The relative muddy cycles from HFS1 to HFS5 are the unfilled setting, and the transgressive flooding surface at the lower part of HFS1 is probably the sequence boundary, resulted from rapid creation of accommodation space. Based on the progradational stacking pattern, the accommodation created by eustatic sea-level rise is a bit smaller than the sediment supply. Sandy cycles from HFS6 to HFS12 are the filled phase, deposited during tectonic pulse, with sediment gradually filling accommodation space and leading to a shallowing-upward sequence. During this period, the extension of the ancient Tethys Sea and related marine flooding gradually ceased. An almost-vertical ascending shoreline trajectory and aggradational stacking patterns suggest that sediment supply increased significantly and overwhelmed the accommodation created by the rising sea level. Conglomerate facies of an alluvial fan system overlying S5 is an overfilled phase, suggesting that accommodation space created by the extension of the ancient Tethys Sea and related marine flooding is totally consumed by high sediment supply.

(2) Detrital modes of sandstone shows that Donghe Sandstone is directly sourced from recycled orogeny. The low content of feldspar and volcanic rock fragments indicates that Donghe Sandstone is recycled from sediment with a cratonic ultimate source. Orogenic activities and linked increasing sediment supply is probably the main driver of Donghe Sandstone S5 and sea-level acted as a secondary factor. Although the allogenic processes such as tectonic, linked increasing sediment supply, and sea level are the potential drivers of stacking patterns of cycles within S5, the autoretreat is an alternative explanation of cycles stacking patterns evidenced by rising sealevel.

(3) Upper shoreface is the most desirable facies for hydrocarbon exploration because it has the best reservoir quality especially highest permeability compared with foreshore, lower shoreface, and offshore transition. Lateral continuity sweet spots are more dominant in the lower part of each HFS from HFS6 to HFS12, which is controlled by the facies stacking pattern, and the facies stacking pattern is ultimately controlled by HFS. During the study of Donghe Sandstone reservoirs, HFS acted as an important tool to evaluate and even predict the vertical and lateral distribution of sweet spots.

(4) This study establishes the relationship between high-frequency sequence stratigraphy with reservoir qualities. The practical application is that high-frequency sequence stratigraphy can predict facies, grain size, grain sorting, and ductile and brittle mineral distribution in order to locate the sweet spots and help engineers on the perforation strategy. This study builds relationships

between high frequency sequence stratigraphy and reservoir characterization and will have implication for the hydrocarbon recovery from clastic shallow-marine reservoirs elsewhere.

Acknowledgements

We would like to thank Dr. Wei Xiong for discussion on facies analysis. Thanks for Dr. Zhang Jinyu for reviewing the manuscript and suggestions. We are grateful for the data analysis from Institute of Porous Flow and Fluid Mechanics of Chinese Academy of Sciences. This research is funded by the PetroChina Tarim Oilfield Branch.

Manuscript received Mar. 21, 2017

accepted Jan. 15, 2018

edited by Hao Qingqing

References

- Ajdukiewicz, J.M., and Lander, R.H., 2010. Sandstone reservoir quality prediction: The state of the art. *AAPG Bulletin*, 94(8): 1083–1091.
- Al-Ramadan, K., Morad, S., Proust, J.N., and Al-Aasm, I.S., 2005. Distribution of diagenetic alterations in siliciclastic shoreface deposits within a sequence stratigraphic framework: evidence from the Upper Jurassic, Boulonnais, NW France. *Journal of Sedimentary Research*, 75(5): 943–959.
- Aminul Islam, M., 2009. Diagenesis and reservoir quality of Bhuban sandstones (Neogene), Titas Gas Field, Bengal Basin, Bangladesh. *Journal of Asian Earth Sciences*, 35(1): 89–100.
- Amorosi, A., Centineo, M.C., Colalongo, M.L., and Fiorini, F., 2005. Millennial-scale depositional cycles from the Holocene of the Po Plain, Italy. *Marine Geology*, 222–223: 7–18.
- Blum, M.D., and Hattier-Womack, J., 2009. Climate change, sea-level change, and fluvial sediment supply to deepwater depositional systems. *External Controls on Modern Clastic Turbidite Systems*: SEPM, Special Publication, 92: 15–39.
- Carvajal, C.R., and Steel, R.J., 2006. Thick turbidite successions from supply-dominated shelves during sea-level highstand. *Geology*, 34(8): 665–668.
- Cattaneo, A., and Steel, R.J., 2003. Transgressive deposits: a review of their variability. *Earth-Science Reviews*, 62(3–4): 187–228.
- Catuneanu, O., Abreu, V., Bhattacharya, J.P., Blum, M.D., Dalrymple, R.W., Eriksson, P.G., Fielding, C.R., Fisher, W.L., Galloway, W.E., Gibling, M.R., Giles, K.A., Holbrook, J.M., Jordan, R., Kendall, C.G.S.C., Macurda, B., Martinsen, O.J., Miall, A.D., Neal, J.E., Nummedal, D., Pomar, L., Posamentier, H.W., Pratt, B.R., Sarg, J.F., Shanley, K.W., Steel, R.J., Strasser, A., Tucker, M.E., and Winker, C., 2009. Towards the standardization of sequence stratigraphy. *Earth-Science Reviews*, 92(1–2): 1–33.
- Catuneanu, O., and Zecchin, M., 2013. High-resolution sequence stratigraphy of clastic shelves II: controls on sequence development. *Marine and Petroleum Geology*, 39(1): 26–38.
- Cheng Yongsheng, 2015. Recent trends on high resolution sequence stratigraphy of shale gas reservoir in China. *Acta Geologica Sinica (English Edition)*, 89(s1): 16–17.
- Coe, A.L., 2003. *The sedimentary record of sea-level change*. Cambridge: Cambridge University Press, 288.
- Coleman, J.M., 1988. Dynamic changes and processes in the Mississippi River delta. *Geological Society of America Bulletin*, 100(7): 999–1015.
- Cross, T.A., 1988. Controls on coal distribution in transgressive-regressive cycles, Upper Cretaceous, Western Interior, USA, in: Wilgus, C.K., Hastings, B.S., Kendall, C.G.S.C., Posamentier, H.W., R., C.A., Van Wagoner, J.C. (Eds.), *Sea Level Changes: An Integrated Approach*. SEPM Special Publication, 42: 371–380.
- Dickinson, W.R., 1985. Interpreting provenance relations from detrital modes of sandstones, in: Zuffa, G.G. (Ed.), *Provenance of arenites: Proceeding of the NATO Advanced Study Institute on Reading Provenance from Arenites*. Springer, Cosenza, Italy, 148: 333–362.
- Dickinson, W.R., Beard, L.S., Brakenridge, G.R., Erjavec, J.L., Ferguson, R.C., Inman, K.F., Knepp, R.A., Lindberg, F.A., and Ryberg, P.T., 1983. Provenance of North American Phanerozoic sandstones in relation to tectonic setting. *Geological Society of America Bulletin*, 94(2): 222–235.
- Dickinson, W.R., and Suczek, C.A., 1979. Plate tectonics and sandstone compositions. *AAPG Bulletin*, 63(12): 2164–2182.
- Dickinson, W.R., and Valloni, R., 1980. Plate settings and provenance of sands in modern ocean basins. *Geology*, 8(2): 82–86.
- dos Anjos, S.M., De Ros, L.F., de Souza, R.S., de Assis Silva, C.M., and Sombra, C.L., 2000. Depositional and diagenetic controls on the reservoir quality of Lower Cretaceous Penedencia sandstones, Potiguar rift basin, Brazil. *AAPG Bulletin*, 84(8): 1719–1742.
- Einsele, G., Ricken, W., and Seilacher, A., 1991. *Cycles and events in stratigraphy*. Berlin: Springer-Verlag, 955.
- Fairbanks, M.D., Ruppel, S.C., and Rowe, H., 2016. High-resolution stratigraphy and facies architecture of the Upper Cretaceous (Cenomanian–Turonian) Eagle Ford Group, Central Texas. *AAPG Bulletin*, 100(3): 379–403.
- Frakes, L.A., and Francis, J.E., 1988. A guide to Phanerozoic cold polar climates from high-latitude ice-rafting in the Cretaceous. *Nature*, 333(6173): 547–549.
- Frakes, L.A., Francis, J.E., and Syktus, J.I., 1992. *Climate modes of the Phanerozoic*. Cambridge: Cambridge University Press, 274.
- Galloway, W.E., 1989. Genetic stratigraphic sequences in basin analysis I: architecture and genesis of flooding-surface bounded depositional units. *AAPG Bulletin*, 73(2): 125–142.
- Guo Wei, Liu Honglin, Xue Huaqing, Lan Chaoli and Tang Xiaoqi, 2015. Depositional facies of Permian Shanxi Formation gas shale in the northern Ordos Basin and its impact on shale reservoir. *Acta Geologica Sinica*, 89(5): 931–941 (in Chinese with English abstract).
- Guo, Z.J., Yin, A., Robinson, A., and Jia, C.Z., 2005. Geochronology and geochemistry of deep-drill-core samples from the basement of the central Tarim Basin. *Journal of Asian Earth Sciences*, 25(1): 45–56.
- Hampson, G.J., 2016. Towards a sequence stratigraphic solution set for autogenic processes and allogenic controls: Upper Cretaceous strata, Book Cliffs, Utah, USA. *Journal of the Geological Society*, 173(5): 817–836.
- Hays, J.D., Imbrie, J., and Shackleton, N.J., 1976. Variations in the Earth's orbit: pacemaker of the ice ages. *Science*, 194

- (4270): 1121–1132.
- Hessler, A. M., Zhang, J., Covault, J., and Ambrose, W., 2017. Continental weathering coupled to Paleogene climate changes in North America. *Geology*, 45(10): 911–914.
- Huang, B., Xu, B., Zhang, C., Li, Y.A., and Zhu, R., 2005. Paleomagnetism of the Baiyisi volcanic rocks (ca. 740Ma) of Tarim, Northwest China: a continental fragment of Neoproterozoic Western Australia? *Precambrian Research*, 142(3): 83–92.
- Jackson, M.D., Hampson, G.J., and Sech, R.P., 2009. Three-dimensional modeling of a shoreface-shelf parasequence reservoir analog: Part 2. Geologic controls on fluid flow and hydrocarbon recovery. *AAPG Bulletin*, 93(9): 1183–1208.
- Jia, D., Lu, H., Cai, D., Wu, S., Shi, Y., and Chen, C., 1998. Structural features of northern Tarim Basin: implications for regional tectonics and petroleum traps. *AAPG Bulletin*, 82(1): 147–159.
- Kidwell, S.M., 1997. Anatomy of extremely thin marine sequences landward of a passive-margin hinge zone; Neogene Calvert Cliffs succession, Maryland, USA. *Journal of Sedimentary Research*, 67(2): 322–340.
- Koo, W.M., Olariu, C., Steel, R.J., Olariu, M.I., Carvajal, C.R., and Kim, W., 2016. Coupling between shelf-edge architecture and submarine-fan growth style inasupply-dominated margin. *Journal of Sedimentary Research*, 86(6): 613–628.
- Lai Jin, Wang Guiwen, Wang Di, Zhou Zhenglong, Ran Ye, Chen Jing, Wang Shuchen and Zhang Xiaotao, 2016. The diagenetic sequence stratigraphy characteristics of Upper Triassic Xujiahe Formation in central Sichuan Basin. *Acta Geologica Sinica*, 90(6): 1236–1252 (in Chinese with English abstract).
- Leckie, D.A., and Walker, R.G., 1982. Storm-and tide-dominated shorelines in Cretaceous Moosebar-Lower Gates interval-outcrop equivalents of Deep Basin gas trap in western Canada. *AAPG Bulletin*, 66(2): 138–157.
- Li, Weiqiang, Taiju Yin, Lun Zhao and Liangdong Zhao, 2017. Distribution patterns of remaining hydrocarbons controlled by reservoir architecture of distributary channel with different channel Style: S2 Formation of Songliao Basin, China. *Acta Geologica Sinica* (English Edition), 91(supp. 1): 129–130.
- Liu Xixiang, Ding Xiaoqi, Zhang Shaonan and He Hao, 2017. Origin and depositional model of deep-water lacustrine sandstone deposits in the 7th and 6th members of the Yanchang Formation (Late Triassic), Binchang area, Ordos Basin, China. *Petroleum Science*, 14(1): 24–36.
- Liu Junlong, Yin Wei, Ji Youliang, Wang Tianyun, Huang Fuxiang, Yu Haiyue and Li Wenshu, 2018. Sequence architecture and sedimentary characteristics of a Middle Jurassic incised valley, western Sichuan depression, China. *Petroleum Science*, 15(2): 230–251.
- Lu, S., Li, H., Zhang, C., and Niu, G., 2008. Geological and geochronological evidence for the Precambrian evolution of the Tarim Craton and surrounding continental fragments. *Precambrian Research*, 160(1): 94–107.
- Luo, X., Hu, C., Xiao, Z., Zhao, J., Zhang, B., Yang, W., Zhao, H., Zhao, F., Lei, Y., and Zhang, L., 2015. Effects of carrier bed heterogeneity on hydrocarbon migration. *Marine and Petroleum Geology*, 68, Part A: 120–131.
- Martins-Neto, M.A., and Catuneanu, O., 2010. Rift sequence stratigraphy. *Marine and Petroleum Geology*, 27(1): 247–253.
- Maynard, J.B., Valloni, R., and Yu, H.S., 1982. *Composition of modern deep-sea sands from arc-related basins*. Geological Society, London, Special Publications, 10: 551–561.
- Mei Mingxiang and Liu Shaofeng, 2017. The Late Triassic sequence-stratigraphic framework of the upper Yangtze region, South China. *Acta Geologica Sinica* (English Edition), 91(1): 51–75.
- Mitchum, R.M., and Van Wagoner, J.C., 1991. High-frequency sequences and their stacking patterns: sequence-stratigraphic evidence of high-frequency eustatic cycles. *Sedimentary Geology*, 70(2–4): 131–160.
- Muto, T., and Steel, R.J., 1997. Principles of regression and transgression: the nature of the interplay between accommodation and sediment supply: perspectives. *Journal of Sedimentary Research*, 67(6): 997–1000.
- Muto, T., and Steel, R.J., 2002. Role of autoretreat and A/S changes in the understanding of deltaic shoreline trajectory: a semi-quantitative approach. *Basin Research*, 14(3): 303–318.
- Naish, T., and Kamp, P.J., 1997. Sequence stratigraphy of sixth-order (41 ky) Pliocene–Pleistocene cyclothem, Wanganui Basin, New Zealand: a case for the regressive systems tract. *Geological Society of America Bulletin*, 109(8): 978–999.
- Posamentier, H.W., and Allen, G.P., 1999. *Siliciclastic sequence stratigraphy: concepts and applications*. SEPM Concepts in Sedimentology and Paleontology, 210.
- Pulham, A.J., 1989. Controls on internal structure and architecture of sandstone bodies within Upper Carboniferous fluvial-dominated deltas, County Clare, western Ireland. *Geological Society, London, Special Publications*, 41(1): 179–203.
- Rich, J.L., 1951. Three critical environments of deposition, and criteria for recognition of rocks deposited in each of them. *Geological Society of America Bulletin*, 62(1): 1–20.
- Rogers, J.J.W., and Santosh, M., 2003. Supercontinents in Earth History. *Gondwana Research*, 6(3): 357–368.
- Sabbagh Bajestani Mahnaz, Mahboubi Asadollah, Moussavi-Harami Reza, Al-Aasma Ihsan and Nadjafi Mehdi, 2017. Facies analysis and sequence stratigraphy of the Qal'eh Dokhtar Formation (Middle–Upper Jurassic) in the west of Boshrouyeh, East Central Iran. *Acta Geologica Sinica* (English Edition), 91(5): 1797–1819.
- Şengör, A., Natal'in, B., and Burtman, V., 1993. Evolution of the Altaid tectonic collage and Palaeozoic crustal growth in Eurasia. *Nature*, 364(6435): 299–307.
- Shu, L.S., Deng, X.L., Zhu, W.B., Ma, D.S., and Xiao, W.J., 2011. Precambrian tectonic evolution of the Tarim Block, NW China: new geochronological insights from the Quruqtagh domain. *Journal of Asian Earth Sciences*, 42(5): 774–790.
- Stefani, M., and Vincenzi, S., 2005. The interplay of eustasy, climate and human activity in the late Quaternary depositional evolution and sedimentary architecture of the Po Delta system. *Marine Geology*, 222–223: 19–48.
- Swenson, J.B., and Muto, T., 2007. Response of coastal plain rivers to falling relative sea-level: allogenic controls on the aggradational phase. *Sedimentology*, 54(1): 207–221.
- Swift, D., Phillips, S., and Thorne, J., 1991. Sedimentation on continental margins: V.parasequences, In: Swift, D.J.P., Oertel, G.F., Tillman, R.W., Thorne, J.A. (Eds.), *Shelf sand and sandstone bodies: geometry, facies and sequence stratigraphy*. International Association of Sedimentologists, Special Publication, 14: 153–187.
- Syvitski, J.P., and Milliman, J.D., 2007. *Geology, geography,*

- and human's battle for dominance over the delivery of fluvial sediment to the coastal ocean. *The Journal of Geology*, 115 (1): 1–19.
- Tobin, R.C., and Schwarzer, D., 2014. Effects of sandstone provenance on reservoir quality preservation in the deep subsurface: experimental modelling of deep-water sand in the Gulf of Mexico. *Geological Society, London, Special Publications*, 386(1): 27–47.
- Wang Zhaoming, Tian Jun., Shen Yinmin, Zhou Lixia and Wang Zhenyu, 2004. Sedimentary facies of Donghe Sandstone during the Late Devonian to Early Carboniferous in Tarim Basin. *Journal of Palaeogeography*, 6(3): 289–296 (in Chinese with English abstract).
- Xian Benzong, Liu Jianping, Dong Yanlei, Lu Zhiyong, He Yanxin and Wang Junhui, 2017. Classification and facies sequence model of subaqueous debris flows. *Acta Geologica Sinica* (English Edition), 91(2): 751–752.
- Xiao, W., Huang, B., Han, C., Sun, S., and Li, J., 2010. A review of the western part of the Altai: a key to understanding the architecture of accretionary orogens. *Gondwana Research*, 18 (2): 253–273.
- Yang, W., Kominz, M.A., and Major, R.P., 1998. Distinguishing the roles of autogenic versus allogenic processes in cyclic sedimentation, Cisco Group (Virgilian and Wolfcampian), north-central Texas. *Geological Society of America Bulletin*, 110(10): 1333–1353.
- Yin Naxin, Xu Huaimin, WubYiming, Liu Yong, Chen Yizhou, Han Tao, Liu Hua and Yin Yuming, 2014. High resolution sequence stratigraphy and excellent reservoir distribution of the Donghe sandstone reservoir in Tazhong 16 reservoir. *Natural Gas Geoscience*, 25(8): 1172–1180.
- Zecchin, M., 2007. The architectural variability of small-scale cycles in shelf and ramp clastic systems: the controlling factors. *Earth-Science Reviews*, 84(1–2): 21–55.
- Zecchin, M., Caffau, M., and Ceramicola, S., 2016. Interplay between regional uplift and glacio-eustasy in the Croton Basin (Calabria, southern Italy) since 0.45 Ma: a review. *Global and Planetary Change*, 143: 196–213.
- Zecchin, M., Caffau, M., Civile, D., Critelli, S., Di Stefano, A., Maniscalco, R., Muto, F., Sturiale, G., and Roda, C., 2012. The Plio-Pleistocene evolution of the Croton Basin (southern Italy): Interplay between sedimentation, tectonics and eustasy in the frame of Calabrian Arc migration. *Earth-Science Reviews*, 115(4): 273–303.
- Zecchin, M., and Catuneanu, O., 2015. High-resolution sequence stratigraphy of clastic shelves III: applications to reservoir geology. *Marine and Petroleum Geology*, 62: 161–175.
- Zhang Daquan, Li Ming and Zhang Xianshu, 1991. Tectonic divisions and hydrocarbon prospects in North Tarim Basin, In: Jia Runxu (Ed.), *Research of petroleum geology of northern Tarim Basin in China*. Wuhan: China University of Geosciences Press, 17–28 (in Chinese with English abstract).
- Zhang Huiliang, Yang Haijun, ShouJianfeng, Zhang Ronghu, GengZhongxia and Wang Bo, 2009. Sedimentary periods of Donghe sandstone and hydrocarbon exploration in Tarim Basin. *Acta PetroleiSinica*, 30(6): 835–842 (in Chinese with English abstract).
- Zhang, J., Qin, L., and Zhang, Z., 2008. Depositional facies, diagenesis and their impact on the reservoir quality of Silurian sandstones from Tazhong area in central Tarim Basin, western China. *Journal of Asian Earth Sciences*, 33(1): 42–60.
- Zhang, J., Steel, R., and Ambrose, W., 2016. Greenhouse shoreline migration: Wilcox deltas. *AAPG Bulletin*, 100(12): 1803–1831.
- Zhang, J., Steel, R., and Ambrose, W., 2017a. Paleocene Wilcox cross-shelf channel-belt history and shelf-margin growth: Key to Gulf of Mexico sediment delivery. *Sedimentary Geology*, 362:53–65.
- Zhang, J., Steel, R., and Olariu, C., 2017b. What conditions are required for deltas to reach the shelf edge during rising sea level? *Geology*, 45(12):1107–1110.
- Zhang, J., Covault, J., Pyrcz, M., Sharman, G. R., Carvajal, C., and Milliken, K., 2018. Quantifying sediment supply to continental margins: Application to the Paleogene Wilcox Group, Gulf of Mexico: *American Association of Petroleum Geologists Bulletin*, 102(9): 1685–1702.
- Zhu Xiaomin, Zhang Qiang, Zhao Chenglin and LüXueyan, 2004. Sedimentary facies and environmental changes of the Donghe sandstone in central Tarim. *Chinese Journal of Geology*, 1(39): 27–35 (in Chinese with English abstract).

About the first author

WANG Ziyuan, born in 1990 in Songyuan City, Jilin Province, obtained a Ph.D. degree from Peking University in 2018. She obtained a Bachelor of Engineering in China University of Petroleum (Beijing) in 2013. During 2015 to 2017, she was an exchange student studying in Bureau of Economic Geology of Jackson School of Geosciences at the University of Texas at Austin. Her research interest includes clastic reservoir characterization and shallow-marine and deep-water depositional systems. E-mail: ziyuan_wang579@126.com.